



	<b>Experiment title:</b> Deciphering Rembrandt's impasto with multi-modal X-ray diffraction	<b>Experiment number:</b> HG130
<b>Beamline:</b> ID22/ID13	<b>Date of experiment:</b> ID22 from: 14/02/18 to: 16/02/18 ID13 from: 07/05/18 to: 10/05/18	<b>Date of report:</b> 18/10/18
<b>Shifts:</b> 6 (ID22) + 9 (ID13)	<b>Local contact(s):</b> ID22 : W. Mogodi , ID13: M. Rosenthal	<i>Received at ESRF:</i>
<b>Names and affiliations of applicants</b> (* indicates experimentalists): Victor Gonzalez <sup>*,1,2</sup> , Marine Cotte <sup>*,3</sup> , Gilles Wallez <sup>*,4,5</sup> , A. van Loon <sup>2</sup> , W. de Nolf <sup>*,3</sup> , Joris Dik <sup>1</sup>  (1) TU Delft, Department of Materials Science and Engineering - Delft University of Technology (2) Rijksmuseum, Science Department (3) ESRF, the European Synchrotron Radiation Facility (4) Institut de Recherche Chimie Paris - PSL Research University, Chimie ParisTech-CNRS, UMR8247 (5) UFR926, Sorbonne Universités		

The main objective of the project was to gather information on the composition and microstructure of the complex lead-based formulations used by Rembrandt to achieve specific pictorial results in his late paintings. More specifically, the technique of impasto (thick paint laid on the canvas in an amount that makes it stand from the surface) was investigated.

To achieve impasto, Rembrandt used the lead white pigment (mix of hydrocerussite  $\text{Pb}_3(\text{CO}_3)_2(\text{OH})_2$  (**HC**) and cerussite  $\text{PbCO}_3$  (**C**)) combined with organic medium (linseed oil). However, the precise recipe that the Master used from those constituents remained unknown.

Using a combination of High-angle resolution (ID22 beamline) and high-lateral resolution XRD to obtain XRPD mapping at the micro-scale (ID13), our objectives were to :

- i) Precisely quantify the crystalline phases constituting Rembrandt's *impastos*.
- ii) Model the pigment crystallites morphology and size for each crystalline phase by Rietveld refinement.
- iii) Obtain crystalline phase distribution maps at the microscale in order to discriminate between different Pb-based phases within the same paint stratification, or modifications of the pigment's composition due to interactions with the binder

## Methods

### A) High-angle resolution XRD (ID22)

The versatility of the ID22 HR-XRD beamline allowed us to select a wavelength of  $\lambda = 0.35420088 \text{ \AA}$ . This wavelength was chosen after preliminaries tryouts : it permitted the obtention of a good compromise to render a good peak resolution, and a sufficient data collection.

Beam size was  $1 \times 1 \text{ mm}^2$ . This surface allowed a global analysis of the entirety of each sample, once they were correctly aligned with the beam. Each recording was constituted by an accumulation of successive diffractograms, on an angular range  $[2^\circ, 20^\circ(2\theta)]$ . Analysis times extended from 1 to 4 hours, according to the amount of diffracting matter contained in the capillary (that is to say, the size of the sample).

### B) High-lateral resolution XRD (ID13)

$\mu$ XRD maps were acquired at the ID13 “microbranch” beamline (ESRF). Samples were either thin ( $10 \mu\text{m}$ ) sections or thick sections, of paint fragments embedded in resin. Samples were mounted vertically, perpendicular to the X-ray beam. The energy of the incident beam was  $13.0 \text{ keV}$ . The beam was focused to  $1.5 \mu\text{m ver.} \times 2.2 \mu\text{m hor.}$  XRD maps were obtained by raster scanning the samples and collecting XRD 2D patterns, in transmission, with the Dectris Eiger 4M single photon counting. 2D XRD patterns were azimuthally integrated using the PyFAI software package and XRD maps were analysed with the XRDUA and the PyMca ROI imaging software packages.

## Results

### A) High-angle resolution XRD (ID22)

Five small paint fragments (one from a ground layer, one from an underlayer paint layer and three from impasto layers) were analyzed (bulk) at ID22. XRD patterns revealed the presence of HC and C in the ground/underlayer samples, as expected. More surprisingly, plumbonacrite  $\text{Pb}_5(\text{CO}_3)_3\text{O}(\text{OH})_2$  (PN) was detected but specifically in impasto samples ( $> 20 \text{ wt\%}$ ). PN is extremely rare in historic paint layers: its presence in artworks dating before the 19<sup>th</sup> c. had never been reported so far. It is notably absent in the large corpus ( $> 35$ ) of historical lead white paints recently studied at the ESRF [1]. Another interesting result was the marginal amount ( $< 10 \text{ wt\%}$ ) of C in these samples, with HC as the main crystalline phase (proportions of different phases are presented in table within Fig. 1). For one sample (Portrait of Marten Soolmans), very high quality HR-XRD patterns were collected by cumulating acquisitions over 4 h. Rietveld refinement was then performed and permitted to achieve modelling of the crystallites morphologies and sizes at the nanometric scale. For PN, the crystallite length in the c axis ( $l_c$ ) is  $\sim 10 \text{ nm}$ . Conversely, the HC crystals in the same impasto paint were significantly larger ( $l_c \sim 100 \text{ nm}$ ) (Fig 1).

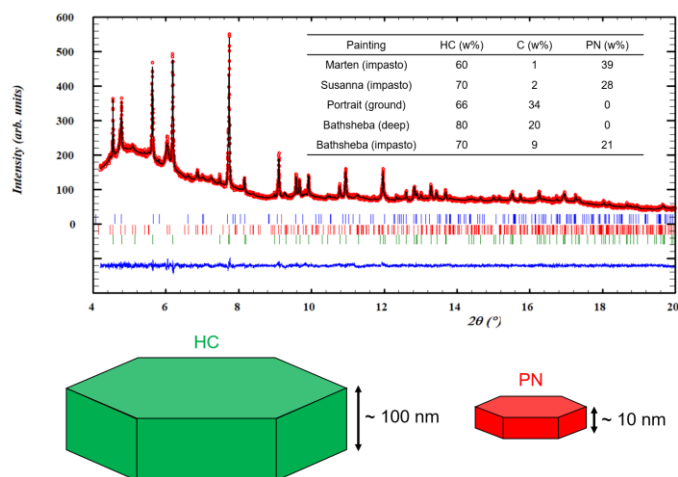


Figure 1 : top) Rietveld plot for sample from the Portrait of Marten Soolmans: experimental (red circles), calculated (black line), difference (blue line), Bragg positions for C (blue), HC (red) and PN (green) containing the weight percentages for HC, C, PN. bottom) Mean dimensions of HC and PN crystallites, produced after Rietveld refinement of the sample

## B) High-lateral resolution XRD (ID13)

Among the samples analyzed at ID13, one was exceptional, as it presented both the lead white impasto layer on top of a lower lead white layer (Fig. 2a). HC was detected in both layers, C only in the lower paint layer and PN specifically in the impasto (Fig 2b). This confirmed the unique phase composition of impastos. Moreover, other maps more precisely revealed the distribution of tiny ( $\sim 5 \mu\text{m}$ ) aggregates of PN crystals homogeneously throughout the impasto layer (Fig 2c,d).

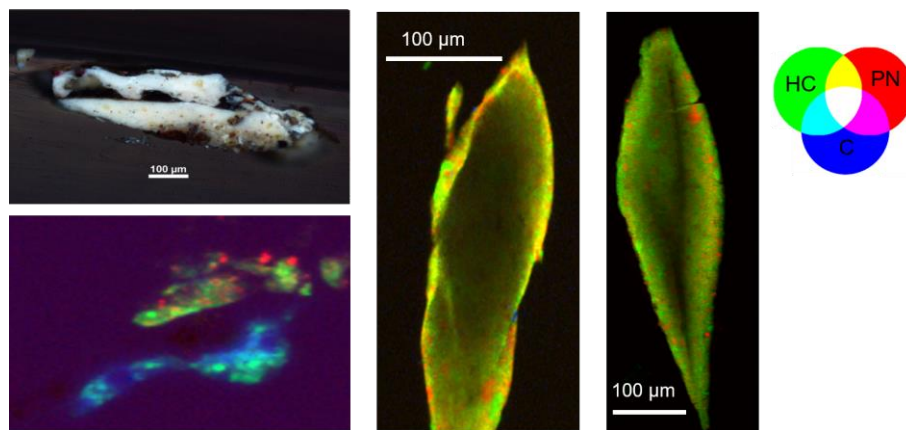


Figure 2 : a) Microscope image of the Bathsheba sample prepared as a polished cross-section (resin block), showing two white layers: impasto on top of an underlayer. b)  $\mu$ -XRD phase maps acquired on a thin section from the Bathsheba sample. c, d)  $\mu$ -XRD phase maps acquired from a cross-section from the thickly painted rosette in the Portrait of Marten Soolmans (c) and from the white drapery of Susanna (d).

## Conclusion and perspectives

The results of this beamtime yielded very important results allowing new insights into the artistic process of Rembrandt, notably :

- The composition and microstructure of Rembrandt's lead white *impastos* differ from other lead white-containing paints in his paintworks, i.e. there was a particular painting technique used to achieve this effect.
- Microscopic proof of crystallisation processes taking place within impasto paint layers was provided.

More specifically, our main hypothesis to explain the presence of this unusual phase is a neo-formation within the impasto layers, in alkaline conditions. The homogeneous dispersion of **PN** under the form of nanometric crystals points to this phenomenon.

This strongly suggest that Rembrandt mastered the rheology of paint in his impastos by the use of an alkaline lead-based medium, possibly by the use of litharge (PbO) treated oil. **PN** could result from the carbonation of PbO drier and/or from the alkalization of **C** and **HC** from the lead white pigment.

All the results of this beamtime were recently detailed in a publication [2].

This research is still on-going today, with the reconstruction of specific impasto-like samples, prepared and aged them under CO<sub>2</sub> rich and CO<sub>2</sub> free atmospheres (to assess the origin of carbonates) and in humid and dry conditions (to assess the effect of water of the phase transformation). Furthermore, we plan to analyse using Synchrotron radiation other lead white/ impasto samples from other paintings by Rembrandt and from other 17th Dutch Masters, in order to increase the studied corpus.

## References

- [1] V. Gonzalez, G. Wallez, T. Calligaro, M. Cotte, W. De Nolf, M. Eveno, E. Ravaud, M. Menu, Anal. Chem., 2017, 89(4), 13203-13211
- [2] V. Gonzalez, M. Cotte, G. Wallez, A. van Loon, W. De Nolf, M. Eveno, K. Keune, P. Noble, J. Dik, Angew. Chem. Int. Ed. 2019, 58, 1 – 5